Published in final edited form as:

Biomacromolecules. 2019 May 13; 20(5): 2115–2122. doi:10.1021/acs.biomac.9b00328.

Acute B-Cell Inhibition by Soluble Antigen Arrays is Valency-Dependent and Predicts Immunomodulation in Splenocytes

J. Daniel Griffin[1], **Martin A. Leon**[2], **Jean R. Salash**[3], **Michael Shao**[4], **Brittany L. Hartwell**[1], **Chad J. Pickens**[3], **Joshua O. Sestak**[3], **Cory Berkland**[1,3,4]

[1]Bioengineering Graduate Program, University of Kansas, Lawrence, KS

[2]Department of Chemistry, University of Kansas, Lawrence, KS

[3]Department of Pharmaceutical Chemistry, University of Kansas, Lawrence, KS

[4]Department of Chemical and Petroleum Engineering, University of Kansas, Lawrence, KS

Abstract

Antigen valency plays a fundamental role in directing the nature of an immune response to be stimulatory or tolerogenic. Soluble Antigen Arrays (SAgAs) are an antigen-specific immunotherapy that combats autoimmunity through the multivalent display of autoantigen. While mechanistic studies have shown SAgAs to induce T and B-cell anergy, the effect of SAgA valency has never been experimentally tested. Here, SAgAs of discrete antigen valencies were synthesized by click chemistry and evaluated for acute B-cell signaling inhibition as well as downstream immunomodulatory effects in splenocytes. Initial studies using the Raji B-cell line demonstrated SAgA valency dictated the extent of calcium flux. Lower valency constructs elicited the largest reductions in B-cell activation. In splenocytes from mice with experimental autoimmune encephalomyelitis, the same valency-dependent effects were evident in the downregulation of the costimulatory marker CD86. The reduction of calcium flux observed in Raji B-cells correlated strongly with downregulation in splenocyte CD86 expression after 72 hours. Here, a thorough analysis of SAgA antigenic valency illustrates that low, but not monovalent, presentation of autoantigen was ideal for eliciting the most potent immunomodulatory effects.

Graphical Abstract

*Corresponding author: berkland@ku.edu; 2030 Becker Drive, Room 320E, Lawrence, KS 66047.

SUPPORTING INFORMATION

Supporting information is available. Figures include HPLC quantification of peptide conjugation, flow cytometry analysis, additional healthy splenocyte data, and raw cytokine results.

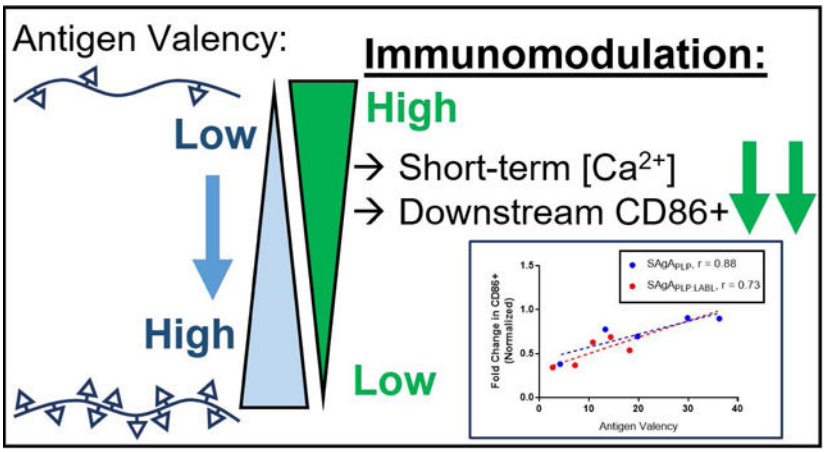

Keywords

Soluble Antigen Array; Antigen-Specific Immunotherapy; Valency; Calcium Flux; Anergy; Click Chemistry

INTRODUCTION

Antigen presentation, especially with regards to valency (the number of antigens presented) can be a powerful therapeutic tool for either stimulating or suppressing immunity. More importantly, tuning ligand density on a macromolecule or colloid can vastly amplify or diminish immune signaling down either pathway[1–5]. Targeting antigen-specific cell surface receptors may also provide a targeted approach to directing immune responses. Moving from monovalent antigen toward a multivalent antigen display can increase therapeutic potency by virtue of increasing receptor engagement through avidity[6–9]. Investigation of both density and valency-dependent immunity matured in the late 1970s with seminal work by Howard Dintzis which illustrated starkly different immunological outcomes. By tuning properties including molecular size and ligand valency, Dintzis observed that large (>100 kD) polymers grafted with high ligand density (>20 ligands/polymer, or 1 ligand per 5 kD) were immunogenic while smaller constructs (<100 kD) with similar or lower valency (<20 ligands/polymer) tended to be tolerogenic in nature[10–13].

Central to this work was a focus on B-cells as potent directors of immunity. Nanoparticles target dendritic cells through nonspecific uptake that is mainly due to transport phenomena where depot formation at injection sites necessitates active transport by these sentinels to secondary lymphoid organs[14–17], but antigen-grafted polymers are uniquely able to target antigen-specific B-cell receptors by virtue of solubility (facilitating passive transport to B-cell rich lymph nodes), backbone flexibility, and retained ligand functionality[18]. Much has been done to elucidate the signaling events triggered by occupation of B-cell receptors (BCR), especially in the area of valency-dependent receptor clustering[19–20]. Work by Kiessling and others has shown BCR clustering events as determinants of cell response, which has reflected many of Dintzis' findings regarding the relationship between valency and immunogenicity[18, 21]. For example, increased avidity afforded by multivalent ligands

was linked to the degree of BCR clustering as a driving factor dictating the B-cell response[22–23]. B-cells are known to be potent initiators of immunity[24], and the successful treatment of autoimmunity through depletion of these populations has reinforced their pathological role in directing the broader immune system[25–27].

Soluble Antigen Arrays (SAgAs) exhibit size and valency characteristics of tolerogenic compounds espoused by Dintzis and others. SAgAs are constructed using antigenic peptides conjugated to a linear, polymeric hyaluronic acid (HA) backbone as antigen-specific immunotherapy (ASIT) for combating autoimmunity[28–29]. Initially SAgAs were developed as a platform for displaying antigen alongside inhibitors of inflammatory immune responses[30–33], though recent mechanistic work has suggested the inhibitors may be somewhat dispensable. These studies have illustrated the integral role of antigen-specific binding and clustering of BCRs for effect[34–36]. Past work has focused almost exclusively on SAgAs made using a 16–20 kD HA backbone displaying roughly 10 copies of antigenic peptide ($PLP_{139–151}$) and 10 copies of a peptide (LABL) that inhibits binding of intracellular cell-adhesion molecule-1 (ICAM-1)[37]. This work has gone far to expand our understanding of how multivalent polymers evoke immunological tolerance through the antigen-specific binding and clustering of BCRs[34–36]. Past studies have shown these events anergize B cells by decreasing calcium flux, downregulating costimulatory molecule CD86 and skewing cytokines toward a regulatory phenotype[35]. Notably, valency has never been experimentally probed in this system where this avid engagement of B cells and clustering of BCRs has been identified as a central to the SAgA mechanism.

Here, we hypothesized that titrating peptide valency could modulate initial B-cell behavior and ultimately tune downstream cellular immune responses in mixed splenocytes. To investigate this supposition, we modified a 16 kD hyaluronic acid backbone and employed click chemistry[38–39] to synthesize a small library of SAgAs with discrete valencies for evaluation in both a B-cell *in vitro* model as well as an *ex vivo* experimental autoimmune encephalomyelitis (EAE) splenocyte assay. Furthermore, we tested the contribution of LABL as a secondary adhesion ligand by investigating the effects of SAgAs conjugated with only $PLP_{139–151}$ antigen as well as those conjugated with both $PLP_{139–151}$ and LABL.

METHODS

Materials

Hyaluronic acid (HA) sodium salt (MW 16 kDa) was purchased from Lifecore Biomedical (Chaska, MN). 11-azido-3,6,9-trioxaundecan-1-amine (NH_2-PEG_3-N_3), *N*-hydroxysuccinimide, *N*-(3-dimethylaminopropyl)-N′-ethylcarbodiimide hydrochloride (EDC), 2-(*N*-morpholino)ethane-sulfonic acid sodium salt (MES), tris(3-hydroxypropyltriazolylmethyl)amine, and sodium ascorbate (NaAsc) were purchased from Sigma-Aldrich (St. Louis, MO). Copper(II) sulfate pentahydrate ($CuSO_4 \cdot 5H_2O$) was purchased from Acros Organics (Geel, Belgium). Alkyne-functionalized peptides with an *N*-terminal 4-pentynoic acid (homopropargyl, hp) modification, $hpPLP_{139–151}$ (hp-HSLGKWLGHPDKF-OH) and hpLABL (hp-ITDGEATDSG-OH) were purchased from Biomatik (Cambridge, ON, Canada). Unmodified $PLP_{139–151}$ (NH2-HSLGKWLGHPDKF-OH) used for rechallenge was purchased from PolyPeptide Laboratories (San Diego, CA).

Fluo-4 AM was purchased from Thermo Fisher Scientific (Waltham, MA). Raji B-cells were obtained from American Type Culture Collection (ATCC, Manassas, VA). Affinity purified F(ab')2 fragment goat anti-human IgM was purchased from Jackson ImmunoResearch Laboratories (West Grove, PA). Incomplete Freund's adjuvant (IFA) and killed *Mycobacterium tuberculosis* strain H37RA were purchased from Difco (Sparks, MD). Pertussis toxin was purchased from List Biological Laboratories (Campbell, CA). R-phycoerythrin (PE)/Cy7-conjugated anti-mouse CD3, PE-conjugated anti-mouse CD86, FITC-conjugated anti-mouse CD80, and respective isotype control antibodies were purchased from BioLegend (San Diego, CA). All other chemicals and reagents were analytical grade and used as received.

Synthesis and Characterization of Varied Valency Conjugates

$SAgA_{PLP}$ and $SAgA_{PLP:LABL}$ were synthesized using click chemistry as previously reported[35], where varied valency was attained by varying reactant hpPLP and hpLABL equivalents per HA-azide and assessing conjugation by RPHPLC. Briefly, a two-step procedure was used to synthesize the conjugates used in this study. 16 kD sodium hyaluronate was reacted with 3-(ethyliminomethyleneamino)-N,N-dimethylpropan-1-amine (EDC) and N-hydroxysuccinimide (NHS) before the addition of $H_2N\text{-}PEG_3\text{-}N_3$. The product was dialyzed and lyophilized to yield hyaluronan-$PEG_3\text{-}N_3$ (HA). $hpPLP_{139–151}$ and/or hpLABL were reacted with azide-modified HA in 50 mM phosphate buffer at room temperature over 24h in the presence of tris(3-hydroxypropyltriazolylmethyl)amine (THPTA), copper (II) sulfate pentahydrate ($CuSO_4{\cdot}5H_2O$), and sodium ascorbate (NaAsc). SAgAs were analyzed quantitatively by RP-HPLC to assess target conjugation efficiencies (Supp. Fig. 1).

Raji B Cell Culture

Raji B-cells were cultured in RPMI-1640 media with L-glutamine, 10% fetal bovine serum (FBS), and 1% penicillin/streptomycin (P/S) at 37 °C and 5% CO_2. Calcium flux was performed only after cells reached confluency after 2 weeks of culture and before 8 passages were reached. Cells were split 1:10 once every 3 days, and calcium flux was performed on the second day after splitting (Raji B-cells in saturated culture at day 3 did not consistently respond to IgM stimulation).

Calcium Flux Experiments

Calcium flux experiments were conducted as previously reported by our group[36]. Briefly, Raji B-cells were loaded with 5 μM Fluo-4 for 30 minutes at room temperature. Cells were washed and resuspended in Hank Balanced Salt Solution (HBSS) before establishing a baseline fluorescence level on the flow cytometer for 60s. Raji B-cells were stimulated with 20 μg/mL goat anti-human IgM, and stimulated fluorescence was measured for another 60s. Stimulated cells were then treated with varied valency conjugates (dosed on a 353.18 μM PLP basis), and fluorescence was read for an additional 180s. Data were analyzed by FlowJo, Kaluza, and GraphPad Prism.

Induction of EAE

EAE was induced as previously described[40–41] in 4–6 week-old, female SJL/J mice from Envigo Laboratories. Mice were housed under specified, pathogen-free conditions at the University of Kansas and under an approved protocol by the University's Institutional Animal Care and Use Committee. EAE was induced by subcutaneously administering mice with 200 μg of PLP in a 0.2 mL emulsion of Complete Freund's Adjuvant (CFA). The CFA mixture was produced from equal volumes of PBS and IFA containing killed Mycobacterium tuberculosis strain H37RA at a final concentration of 4 mg/mL. The immunization was administered as four, 50 μL injections above the shoulders and the flanks. An additional 200 ng of pertussis toxin was given intraperitoneally on the same day of immunization (day 0) as well as day 2 post-immunization. Mice were weighed each day of the study and monitored with clinical scores starting on day 7.

Spleen Harvest and Splenocyte Isolation

Splenocytes were harvested from EAE and healthy control mice at peak of disease (Day 12 post-induction). Spleen harvest and splenocyte isolation was conducted as previously reported[35]. Briefly, spleens were passed through a wire mesh using the rubber stopper of a sterile 1 mL syringe in RPMI-1640 media. The strained cellular extracts were centrifuged, and the cell pellet was resuspended in red blood cell lysis buffer. The cells were incubated on ice for 3.5 minutes to lyse splenic red blood cells. The lysis reaction was stopped by adding 10 mL RPMI 1640 media containing 10% FBS to the mixture before centrifuging. The remaining splenocyte pellets were resuspended in fresh media (RPMI 1640 media containing 10% FBS and 1% Penicillin-Streptomycin) and plated in 24-well cell culture plates at a cell density of 3×10^6 cells/well as well as a 96-well format at 1×10^6 cells/well. Varied valency conjugates were introduced in triplicate (both for EAE and healthy control splenocytes and in two sets per group for flow cytometry and cytokines, respectively) to each well at 141.3 μM to replicate dosing from past studies, as well as 25 μM PLP. Each cell culture was incubated for 72 hours at 37 °C in a CO_2 (5%) incubator.

Fluorescent Staining and Flow Cytometry

Splenocytes were collected from 24-well plates after 72 hours and stained with fluorescent antibodies according to manufacturer recommendations. Cells were washed with 1 mL of RPMI-1640 + 5% FBS before centrifuging and resuspending in 50 μL of 20 μg/mL TruStain fcX blocking antibody (anti-mouse CD16/32 antibody, Biolegend). Cells were incubated on ice for 30 minutes before adding the fluorescent antibodies and isotype controls in 50 μL for 1 hour. For flow cytometry data collection, 30,000 cells per sample were detected using a BD FACSFusion cytometer. Data were analyzed using Kaluza, FlowJo, and GraphPad Prism software.

Measurement of Cytokines

Following the 72-hour incubation, splenocytes in a 96-well culture plate were centrifuged. Supernatants were collected for cytokine analysis (GM-CSF, IFN- γ, IL-2, IL-21, IL-6, IL-10, IL-17, IL-23, TNF-α). Marker levels were detected using a U-Plex assay kit according to manufacturer instructions (Meso Scale Discovery). Briefly, each plate was

coated with 50 μL of multiplex coating solution consisting of linkers and biotinylated capture antibodies for each cytokine and incubated on a shaker at 700 rpm for 1 hour at room temperature. Following a 3X wash step with 150 μL PBS containing 0.05% Tween 20, 25 μL of diluent and 25 μL of sample was added to each well and incubated again for 1 hour on a shaker at room temperature. Detection antibody was then added at 50 μL/well and incubated for 1 hour. Finally, each assay plate was read using the QuickPlex multiplex plate reader (Meso Scale Discovery).

Measurement of Cellular Metabolism.

Resazurin (7-hydroxy-3H-phenoxazin-3-one 10-oxide) was incubated with centrifuged splenocytes leftover from cytokine supernatant collection to determine cellular metabolism. 75 μM resazurin was introduced to splenocyte cultures and incubated for 3 hours. Metabolic reductive capacity was observed by viewing changes in fluorescence at excitation 560, emission 590 (Spectramax M5, Molecular Devices). Background fluorescence were taken using RPMI media and subtracted out from splenocyte readings for analysis.

Statistical Analysis

Statistical evaluation was performed using one- and two-way analysis of variance (ANOVA), followed by Tukey and Sidak multiple comparison tests. Statistical significance for all analyses was set at $p<0.05$. All statistical analyses were performed using GraphPad Software (GraphPad Software Inc.).

RESULTS

Synthesis of Varied-Valency Conjugates.

Soluble antigen arrays displaying antigen ($SAgA_{PLP}$) or antigen plus inhibitor ($SAgA_{PLP:LABL}$) were synthesized by click chemistry using previously described methods[35]. Reactant quantities of PLP and LABL peptides were titrated to yield constructs of varied valency, defined by percent ligand occupancy of the 42 azide-modified sites of a 16 kD HA backbone and calculated by RP-HPLC (Fig. 1, Supp. Fig. 1). $SAgA_{PLP}$ was synthesized in a single batch, where peptide conjugation deviated less than 5% from the desired conjugation efficiencies of 10%, 30%, 50%, 70%, and 90% occupancy. For the $SAgA_{PLP:LABL}$, the same efficiencies were targeted for overall valency, though backbone occupancy was equally divided between PLP and LABL. Single batch synthesis of these constructs maintained conjugation accuracy within 5%, excepting 90% $SAgA_{PLP:LABL}$, where average peptide conjugation peaked at 82%.

Inhibition of Short-Term B-cell Response is Valency-Dependent.

To investigate acute valency-dependent effects of $SAgA_{PLP}$ and $SAgA_{PLP:LABL}$, an immortalized B-cell line (Raji B cells) were loaded with a calcium-indicating fluorochrome and stimulated with anti-IgM fragments[20]. Influx of Ca^{2+} ions to B cells is critical for propagating immunity, and past SAgA studies have demonstrated the inhibition of this stimulatory signaling event[36]. Here, Stimulated B-cells showed distinctly increased peak fluorescence over baseline (Fig 2A). Following SAgA treatment, a brief spike was consistently observed in Fluo-4 signal intensity and monitoring over the course of three

minutes illustrated a net reduction that was normalized against untreated controls (Fig. 2B). The degree of reduction by $SAgA_{PLP}$ and $SAgA_{PLP:LABL}$ varied in a valency-dependent manner (Fig. 2C). In the one-signal $SAgA_{PLP}$ constructs, reduction trended inversely with valency, and the 10% construct elicited a significantly higher reduction in calcium signal than both 70% and 90% $SAgA_{PLP}$. A similar trend was realized in the $SAgA_{PLP:LABL}$ cohort; 10% $SAgA_{PLP:LABL}$ reduced Fluo-4 signal significantly more than 70% and 90% $SAgA_{PLP:LABL}$, while 30%, 50%, and 70% constructs each outperformed 90% $SAgA_{PLP:LABL}$. Between $SAgA_{PLP}$ and $SAgA_{PLP:LABL}$, dosing was maintained on a basis of PLP concentration (*i.e.* the total molar dose of $SAgA_{PLP:LABL}$ was roughly double $SAgA_{PLP}$). For the HA alone control group, molar dose was selected to be equivalent to that of the lowest valency SAgA in this study such that this group would convey the highest relative number of molecules in solution.

Low-Valency Conjugates Induce Downstream Anergy in Mixed EAE Splenocytes.

Next, varied valency conjugates were tested against EAE splenocytes to investigate whether the findings of acute B-cell inhibition could predict outcomes in a more complex system. Splenocytes were harvested from healthy mice and from EAE mice at peak of disease. We incubated cells with a rechallenge of autoantigen epitope $PLP_{139–151}$ to prompt stimulation of antigen-specific immunity in the presence of varied valency SAgAs. After a 72 hour incubation, samples were labeled for costimulatory markers CD86 and CD80 to assess the activation states of antigen-presenting cells (including B-cells). CD3 was also labeled in the panel to probe fluctuations in T cells (Fig. 3, Supp. Fig. 3). This study was conducted in two separate animal experiments, so population changes were reported as normalized to respective vehicle controls for comparison. For both $SAgA_{PLP}$ and $SAgA_{PLP:LABL}$ treatments, valency correlated with CD86 expression at 72 hours. Only low valency conjugates (10% $SAgA_{PLP}$, 10% $SAgA_{PLP:LABL}$ and 30% $SAgA_{PLP:LABL}$) were statistically similar to healthy controls for each replicate, though all SAgAs tested elicited a decreased expression of this costimulatory marker (Fig. 3A). Interestingly, CD80 expression showed the inverse; the same low valency conjugates exhibited the highest CD80 expression, which may have indicated a regulatory phenotype when taken in conjunction with decreased CD86 and higher levels of T cells[42–45]. The 10% $SAgA_{PLP}$ treatment doubled CD80 expression compared to the healthy control, and 10% and 30% $SAgA_{PLP:LABL}$ remained comparable to the healthy control. When comparing the healthy control and all SAgAs, an increase in CD80 expression was consistently observed (Fig. 3B). SAgA treatment generally increased CD3+ populations with the exception of 70% and 90% $SAgA_{PLP}$ (Fig. 3C). Additional analysis of CD86 dot plots for the historically reported, 50% conjugated $SAgA_{PLP:LABL}$ compared with low valency 10% $SAgA_{PLP:LABL}$ revealed substantial CD86 downregulation (Fig. 3D).

Changes in cell metabolism were also investigated in splenocytes treated with varied valency conjugates (Fig. 4). Elevated metabolism is a hallmark of a stimulated immune response, so here we assessed decreases in metabolism to indicate inhibited immunity. The resazurin metabolic assay was employed toward this end, as this compound is reduced to fluorescent resorfurin in the presence of NADH, thus allowing quantification of cell respiration. In EAE splenocytes (Fig. 4A), $SAgA_{PLP}$, but not $SAgA_{PLP:LABL}$ evoked significant decreases in

resazurin metabolism. Notably, in healthy splenocytes (Fig. 4B), only low valency 10% $SAgA_{PLP}$ did *not* increase metabolism, while $SAgA_{PLP:LABL}$ treatment largely did not affect metabolic outcomes. Cytokine analysis was also performed for EAE splenocytes treated with $SAgA_{PLP}$ and $SAgA_{PLP:LABL}$ (Fig. 4C, Supp. Fig. 4). These biomarkers provide signals, which can indicate the stimulatory or tolerogenic nature of an immune response. Interestingly, two distinct signatures were apparent. $SAgA_{PLP}$ was characterized by non-valency discriminate increases in IL-6 and anti-inflammatory Il-10, with a decrease in T cell proliferation suggested by reduced Il-2. However, low valency conjugates elicited smaller increases in Il-17 and Il-12, indicating less inflammation and costimulatory antigen-presentation. Inflammatory Il-17 production was markedly increased by cells treated with $SAgA_{PLP:LABL}$ conjugates, and the cytokines Il-6 and TNF-α increased to a lesser extent.

DISCUSSION

While the number of antigens is an important characteristic for directing the type and magnitude of immune response[1–3], the valency at which antigens are presented along a polymeric backbone requires further exploration. In recent work by Arthur *et al.*, allogenic responses to blood transfusions were exacerbated by red blood cells containing high levels of alloantigen, but stifled by cells engineered to carry a low level of alloantigen[4]. In 2018, the Jewell group showed that quantum dots displaying low antigen density were superior to those loaded with high levels of antigen in terms of evoking tolerance[5]. Interestingly, this work focused on the modulation of dendritic cells as a mechanism, where nonspecific endocytosis drives effect. Certainly, nonspecific dendritic cell modulation was shown to be feasible in our system as well[35], but SAgAs are differentially capable of antigen-specific B-cell receptor engagement by virtue of a flexible, soluble polymeric backbone. In our present study, we evaluated the titration of antigen valency using this system, where distinct antigen-specific modulation of B-cells has been reported in autoimmune disease models[34–36].

The work presented here built from the mechanistic foundations that have positioned B cells as key targets of the SAgA mechanism[34–36]. In past work elucidating these insights, we found SAgAs to be capable of specifically engaging B cells and inhibiting the acute (t = minutes) influx of Ca^{2+} ions necessary to propagate immunity[36]. Later, we found these short-term changes observed *ex vivo* were correlated to *in vivo* efficacy[34]. and *Ex vivo* costimulatory marker downregulation and a humoral skewing of immunity were also correlated to *in vivo* SAgA mechanisms of EAE prevention[35].

Here, both acute-phase (Fig. 2) and downstream response (Fig. 3, Fig. 4) assays showed immunomodulatory outcomes were that were highly dependent on SAgA antigen valency (Fig. 5). For the short-term reduction of calcium signaling in Raji B-cells, both $SAgA_{PLP}$ and $SAgA_{PLP:LABL}$ showed an inverse relationship of similar magnitudes between calcium inhibition and PLP valency (Fig. 5A). Similar trending was observed when mixed EAE splenocytes were treated with SAgAs for 72 hours. CD86+ cells decreased with valency, meaning $SAgA_{PLP}$ and $SAgA_{PLP:LABL}$ of low PLP conjugation translated to the highest reductions of this costimulatory marker (Fig. 5B). Together, these data suggest that low valency, but not monovalent, antigen display is able to evoke the most potent immunosuppressive effects in both the acute and downstream frames of immunity.

Interestingly, $SAgA_{PLP:LABL}$ showed an apparent advantage over $SAgA_{PLP}$ in acute phase calcium inhibition that was not observed in the splenocyte experiments (Fig. 5A). While not statistically definitive, this discrepancy could be due to increased binding avidity afforded by the inclusion of LABL, which may allow $SAgA_{PLP:LABL}$ to engage and persist at the cell surface through binding ICAM-1 in addition to B-cell receptors. This marginal increase in short-term performance does not appear to critical to downstream effect, as CD86 downregulation of $SAgA_{PLP:LABL}$ mirrored $SAgA_{PLP}$ (Fig. 4B). The splenocyte experiment demonstrated a clear valency-dependent trend was maintained wherein the lowest valency $SAgA_{PLP}$ and $SAgA_{PLP:LABL}$ reduced CD86 expression to the greatest extent. Notably, this effect was found to *inversely* trend with CD80, another common marker of costimulation (Fig. 3B). While initially unexpected, reports have indicated CD80 in the absence of CD86, directs inhibition of T cells when regulatory T and B subsets are prevalent[42–45]. The potential for this phenomenon to explain the data we observed is substantiated by an overall increase in T cell populations (possibly reflecting an increase in T_{regs} caused by SAgA treatment, Fig. 3C), though future studies are necessary to evaluate fully.

Generally, incubation of EAE splenocytes with SAgAs led to a decreased metabolism after 72 hours (Fig. 4A). In healthy splenocytes, 10% $SAgA_{PLP}$ and all $SAgA_{PLP:LABL}$ exhibited resazurin levels comparable to vehicle-treated control, but $SAgA_{PLP}$ of valency 30% and higher caused an elevated metabolism. This finding may be due to the higher antigen number of $SAgA_{PLP}$ over $SAgA_{PLP:LABL}$ triggering more immunogenicity, though this change did not translate to a stimulated immune response overall (Supp. Fig. 3). Cytokine responses between $SAgA_{PLP}$ and $SAgA_{PLP:LABL}$ seemed distinct, possibly highlighting a difference in signaling pathways created by the inclusion of LABL (Fig. 4C). In $SAgA_{PLP}$, a robust Il-10 response with the elevation of many other markers was consistent with past work, but the increased Il-17 response in $SAgA_{PLP:LABL}$ treated splenocytes was atypical. Differences in cytokines did not, however, translate to altered cell phenotypes (Fig. 3).

Adding to the valency dependencies outlined in this work, acute B cell calcium flux inhibition was found to be highly correlative of CD86 expression in a mixed population of splenocytes (Fig. 5C). The implication of this observation further substantiates our past investigations of B cells as a key target of SAgAs for effect. While other mechanisms may aid in SAgA efficacy, fold change in calcium flux in this experiment proved informative for long-term (72 hours) outcomes in a more complex, mixed system of splenocytes. Ultimately, correlations between antigen valency, calcium flux reduction, and CD86 expression were all highly significant (Fig. 5D).

CONCLUSIONS

SAgAs were found to be capable of modulating B-cell calcium signaling and mixed splenocyte CD86 expression in a valency-dependent fashion. SAgAs were most effective when antigen valency was low, reflecting Dintzis' "rules" with greater resolution than previously elucidated[46]. SAgAs displaying 4–7 PLP were most effective, overshadowing the conventional, albeit effective SAgA constructs displaying 10 PLP, which have been the focal point of our prior studies. Furthermore, the level of acute B-cell inhibition studied in isolation correlated with downregulation of CD86 in splenocytes. Together, studies indicated

SAgA valency was an important driver of immune response, which casts light on the role of valency when designing antigen-specific immunotherapies.

Supplementary Material

Refer to Web version on PubMed Central for supplementary material.

ACKNOWLEDGEMENTS

JDG and BLH were supported by the Madison and Lila Self Graduate Fellowship at the University of Kansas. Also, authors MAL and CJP gratefully acknowledge support from the National Institutes of Health Graduate Training Program in Dynamic Aspects of Chemical Biology Grant (T32 GM008545) from the National Institutes of General Medical Sciences.

REFERENCES

1. Hartwell BL; Antunez L; Sullivan BP; Thati S; Sestak JO; Berkland C, Multivalent nanomaterials: learning from vaccines and progressing to antigen-specific immunotherapies. J. Pharm. Sci 2015, 104 (2), 346–361. [PubMed: 25447598]
2. Bachmann MF; Jennings GT, Vaccine delivery: a matter of size, geometry, kinetics and molecular patterns. Nat. Rev. Immunol 2010, 10 (11), 787. [PubMed: 20948547]
3. Gestwicki JE; Cairo CW; Strong LE; Oetjen KA; Kiessling LL, Influencing receptor–ligand binding mechanisms with multivalent ligand architecture. J. Am. Chem. Soc 2002, 124 (50), 14922–14933. [PubMed: 12475334]
4. Arthur CM; Patel SR; Smith NH; Bennett A; Kamili NA; Mener A; Gerner-Smidt C; Sullivan HC; Hale JS; Wieland A; Youngblood B; Zimring JC; Hendrickson JE; Stowell SR, Antigen Density Dictates Immune Responsiveness following Red Blood Cell Transfusion. J. Immunol 2017, 198 (7), 2671–2680. [PubMed: 28250159]
5. Hess KL; Oh E; Tostanoski LH; Andorko JI; Susumu K; Deschamps JR; Medintz IL; Jewell CM, Engineering Immunological Tolerance Using Quantum Dots to Tune the Density of Self-Antigen Display. Adv. Funct. Mater 2017, 27 (22), 1700290. [PubMed: 29503604]
6. Minguet S; Dopfer E-P; Schamel WWA, Low-valency, but not monovalent, antigens trigger the B-cell antigen receptor (BCR). Int. Immunol 2010, 22 (3), 205–212. [PubMed: 20145007]
7. Nielsen UB; Adams GP; Weiner LM; Marks JD, Targeting of bivalent anti-ErbB2 diabody antibody fragments to tumor cells is independent of the intrinsic antibody affinity. Cancer Res. 2000, 60 (22), 6434–40. [PubMed: 11103810]
8. Adams GP; Tai M-S; McCartney JE; Marks JD; Stafford WF; Houston LL; Huston JS; Weiner LM, Avidity-Mediated Enhancement of In vivo Tumor Targeting by Single-Chain Fv Dimers. Clin. Cancer Res 2006, 12 (5), 1599–1605. [PubMed: 16533787]
9. Kubetzko S; Balic E; Waibel R; Zangemeister-Wittke U; Pluckthun A, PEGylation and multimerization of the anti-p185HER-2 single chain Fv fragment 4D5: effects on tumor targeting. J. Biol. Chem 2006, 281 (46), 35186–201. [PubMed: 16963450]
10. Dintzis HM; Dintzis RZ; Vogelstein B, Molecular determinants of immunogenicity: the immunon model of immune response. Proc. Natl. Acad. Sci 1976, 73 (10), 3671–3675. [PubMed: 62364]
11. Dintzis RZ; Middleton MH; Dintzis HM, Studies on the immunogenicity and tolerogenicity of T-independent antigens. J. Immunol 1983, 131 (5), 2196–2203. [PubMed: 6631009]
12. Dintzis RZ; Middleton MH; Dintzis HM, Inhibition of anti-DNP antibody formation by high doses of DNP-polyacrylamide molecules; effects of hapten density and hapten valence. J. Immunol 1985, 135 (1), 423–427. [PubMed: 3889155]
13. Dintzis RZ; Okajima M; Middleton M; Greene G; Dintzis H, The immunogenicity of soluble haptenated polymers is determined by molecular mass and hapten valence. J. Immunol 1989, 143 (4), 1239–1244. [PubMed: 2473123]

14. Manolova V; Flace A; Bauer M; Schwarz K; Saudan P; Bachmann MF, Nanoparticles target distinct dendritic cell populations according to their size. Eur. J. Immunol 2008, 38 (5), 1404–1413. [PubMed: 18389478]
15. Reddy ST; Rehor A; Schmoekel HG; Hubbell JA; Swartz MA, In vivo targeting of dendritic cells in lymph nodes with poly (propylene sulfide) nanoparticles. J. Control. Release 2006, 112 (1), 26–34. [PubMed: 16529839]
16. Uto T; Wang X; Sato K; Haraguchi M; Akagi T; Akashi M; Baba M, Targeting of antigen to dendritic cells with poly (γ-glutamic acid) nanoparticles induces antigen-specific humoral and cellular immunity. J. Immunol 2007, 178 (5), 2979–2986. [PubMed: 17312143]
17. Maldonado RA; LaMothe RA; Ferrari JD; Zhang A-H; Rossi RJ; Kolte PN; Griset AP; O'Neil C; Altreuter DH; Browning E; Johnston L; Farokhzad OC; Langer R; Scott DW; von Andrian UH; Kishimoto TK, Polymeric synthetic nanoparticles for the induction of antigen-specific immunological tolerance. Proc. Natl. Acad. Sci 2015, 112 (2), E156–E165. [PubMed: 25548186]
18. Puffer EB; Pontrello JK; Hollenbeck JJ; Kink JA; Kiessling LL, Activating B Cell Signaling with Defined Multivalent Ligands. ACS Chem. Biol 2007, 2 (4), 252–262. [PubMed: 17432821]
19. Fleire SJ; Goldman JP; Carrasco YR; Weber M; Bray D; Batista FD, B Cell Ligand Discrimination Through a Spreading and Contraction Response. Science 2006, 312 (5774), 738–741. [PubMed: 16675699]
20. Minguet S; Klasener K; Schaffer AM; Fiala GJ; Osteso-Ibanez T; Raute K; Navarro-Lerida I; Hartl FA; Seidl M; Reth M; Del Pozo MA, Caveolin-1-dependent nanoscale organization of the BCR regulates B cell tolerance. Nat. Immunol 2017, 18 (10), 1150–1159. [PubMed: 28805811]
21. Cairo CW; Gestwicki JE; Kanai M; Kiessling LL, Control of Multivalent Interactions by Binding Epitope Density. J. Am. Chem. Soc 2002, 124 (8), 1615–1619. [PubMed: 11853434]
22. Kiessling LL; Gestwicki JE; Strong LE, Synthetic multivalent ligands in the exploration of cell-surface interactions. Curr. Opin. Chem. Biol 2000, 4 (6), 696–703. [PubMed: 11102876]
23. Gestwicki JE; Cairo CW; Strong LE; Oetjen KA; Kiessling LL, Influencing Receptor–Ligand Binding Mechanisms with Multivalent Ligand Architecture. J. Am. Chem. Soc 2002, 124 (50), 14922–14933. [PubMed: 12475334]
24. Lund FE; Randall TD, Effector and regulatory B cells: modulators of CD4+ T cell immunity. Nat. Rev. Immunol 2010, 10 (4), 236. [PubMed: 20224569]
25. Franks SE; Getahun A; Hogarth PM; Cambier JC, Targeting B cells in treatment of autoimmunity. Curr. Opin. Immunol 2016, 43, 39–45. [PubMed: 27718447]
26. Liossis S-NC; Sfikakis PP, Rituximab-induced B cell depletion in autoimmune diseases: potential effects on T cells. Clin. Immunol 2008, 127 (3), 280–285. [PubMed: 18337174]
27. Milo R, Therapeutic strategies targeting B-cells in multiple sclerosis. Autoimmun. Rev 2016, 15 (7), 714–718. [PubMed: 26970489]
28. Berkland C; Sestak J; Siahaan T, Bifunctional conjugate compositions and associated methods. Google Patents: 2013.
29. Sestak J; Mullins M; Northrup L; Thati S; Laird Forrest M; Siahaan TJ; Berkland C, Single-step grafting of aminooxy-peptides to hyaluronan: A simple approach to multifunctional therapeutics for experimental autoimmune encephalomyelitis. J. Control. Release 2013, 168 (3), 334–340. [PubMed: 23541930]
30. Sestak JO; Sullivan BP; Thati S; Northrup L; Hartwell B; Antunez L; Forrest ML; Vines CM; Siahaan TJ; Berkland C, Codelivery of antigen and an immune cell adhesion inhibitor is necessary for efficacy of soluble antigen arrays in experimental autoimmune encephalomyelitis. Mol Ther Methods Clin Dev 2014, 1, 14008. [PubMed: 26015953]
31. Hartwell BL; Smalter Hall A; Swafford D; Sullivan BP; Garza A; Sestak JO; Northrup L; Berkland C, Molecular Dynamics of Multivalent Soluble Antigen Arrays Support a Two-Signal Co-delivery Mechanism in the Treatment of Experimental Autoimmune Encephalomyelitis. Mol. Pharm 2016, 13 (2), 330–43. [PubMed: 26636828]
32. Northrup L; Sestak JO; Sullivan BP; Thati S; Hartwell BL; Siahaan TJ; Vines CM; Berkland C, Co-delivery of autoantigen and b7 pathway modulators suppresses experimental autoimmune encephalomyelitis. Aaps j 2014, 16 (6), 1204–13. [PubMed: 25297853]

33. Northrup L; Christopher MA; Sullivan BP; Berkland C, Combining antigen and immunomodulators: Emerging trends in antigen-specific immunotherapy for autoimmunity. Adv. Drug Del. Rev 2016, 98, 86–98.
34. Hartwell BL; Pickens CJ; Leon M; Berkland C, Multivalent Soluble Antigen Arrays Exhibit High Avidity Binding and Modulation of B Cell Receptor-Mediated Signaling to Drive Efficacy against Experimental Autoimmune Encephalomyelitis. Biomacromolecules 2017, 18 (6), 1893–1907. [PubMed: 28474886]
35. Hartwell BL; Pickens CJ; Leon M; Northrup L; Christopher MA; Griffin JD; Martinez-Becerra F; Berkland C, Soluble antigen arrays disarm antigen-specific B cells to promote lasting immune tolerance in experimental autoimmune encephalomyelitis. J. Autoimmun 2018, 93, 76–88. [PubMed: 30007842]
36. Hartwell BL; Martinez-Becerra FJ; Chen J; Shinogle H; Sarnowski M; Moore DS; Berkland C, Antigen-Specific Binding of Multivalent Soluble Antigen Arrays Induces Receptor Clustering and Impedes B Cell Receptor Mediated Signaling. Biomacromolecules 2016, 17 (3), 710–722. [PubMed: 26771518]
37. Yusuf-Makagiansar H; Anderson ME; Yakovleva TV; Murray JS; Siahaan TJ, Inhibition of LFA-1/ICAM-1 and VLA-4/VCAM-1 as a therapeutic approach to inflammation and autoimmune diseases. Med. Res. Rev 2002, 22 (2), 146–167. [PubMed: 11857637]
38. Nandivada H; Jiang XW; Lahann J, Click chemistry: Versatility and control in the hands of materials scientists. Adv. Mater 2007, 19 (17), 2197–2208.
39. Pickens CJ; Johnson SN; Pressnall MM; Leon MA; Berkland CJ, Practical Considerations, Challenges, and Limitations of Bioconjugation via Azide-Alkyne Cycloaddition. Bioconjug. Chem 2018, 29 (3), 686–701. [PubMed: 29287474]
40. Northrup L; Griffin JD; Christopher MA; Antunez LR; Hartwell BL; Pickens CJ; Berkland C, Co-delivery of autoantigen and dexamethasone in incomplete Freund's adjuvant ameliorates experimental autoimmune encephalomyelitis. J. Control. Release 2017, 266, 156–165. [PubMed: 28963036]
41. Griffin JD; Christopher MA; Thati S; Salash JR; Pressnall MM; Weerasekara DB; Lunte SM; Berkland CJ, Tocopherol Emulsions as Functional Autoantigen Delivery Vehicles Evoke Therapeutic Efficacy in Experimental Autoimmune Encephalomyelitis. Mol. Pharm 2019, 16 (2), 607–617. [PubMed: 30615457]
42. Zheng Y; Manzotti CN; Liu M; Burke F; Mead KI; Sansom DM, CD86 and CD80 differentially modulate the suppressive function of human regulatory T cells. J. Immunol 2004, 172 (5), 2778–2784. [PubMed: 14978077]
43. Nova-Lamperti E; Fanelli G; Becker PD; Chana P; Elgueta R; Dodd PC; Lord GM; Lombardi G; Hernandez-Fuentes MP, IL-10-produced by human transitional B-cells down-regulates CD86 expression on B-cells leading to inhibition of CD4+ T-cell responses. Sci. Rep 2016, 6, 20044. [PubMed: 26795594]
44. Manzotti CN; Tipping H; Perry LC; Mead KI; Blair PJ; Zheng Y; Sansom DM, Inhibition of human T cell proliferation by CTLA-4 utilizes CD80 and requires CD25+ regulatory T cells. Eur. J. Immunol 2002, 32 (10), 2888–2896. [PubMed: 12355442]
45. Sansom DM; Manzotti CN; Zheng Y, What's the difference between CD80 and CD86? Trends Immunol. 2003, 24 (6), 313–318.
46. Dintzis RZ; Okajima M; Middleton MH; Dintzis HM, Inhibition of antibody formation by receptor cross-linking: the molecular characteristics of inhibitory haptenated polymers. Eur. J. Immunol 1990, 20 (1), 229–232. [PubMed: 1689663]

Target Conj.			Approx. MW (kDa)	Peptide:HA		TOTAL	
				PLP	LABL	#	%
$SAgA_{PLP}$	10%		31.4	4.2	0	4.2	10%
	30%		46.0	13.3	0	13.3	32%
	50%		56.4	19.8	0	19.8	47%
	70%		72.5	29.9	0	29.9	71%
	90%		82.8	36.3	0	36.3	86%
$SAgA_{PLP:LABL}$	10%		30.9	2.7	1.8	4.5	11%
	30%		41.6	7.2	5.2	12.4	29%
	50%		53.5	10.8	11.1	21.9	52%
	70%		63.0	14.4	14.7	29.1	69%
	90%		71.1	18.2	16.6	34.8	82%
△ - PLP ○ - LABL							

Fig. 1.

Synthesis of varied valency conjugates. Antigen-only ($SAgA_{PLP}$) and antigen plus inhibitor ($SAgA_{PLP:LABL}$) conjugates were synthesized by click chemistry according to varied target conjugation efficiencies for each 16 kD HA backbone. RP-HPLC was used for characterization, and calculated peptide conjugations are reported.

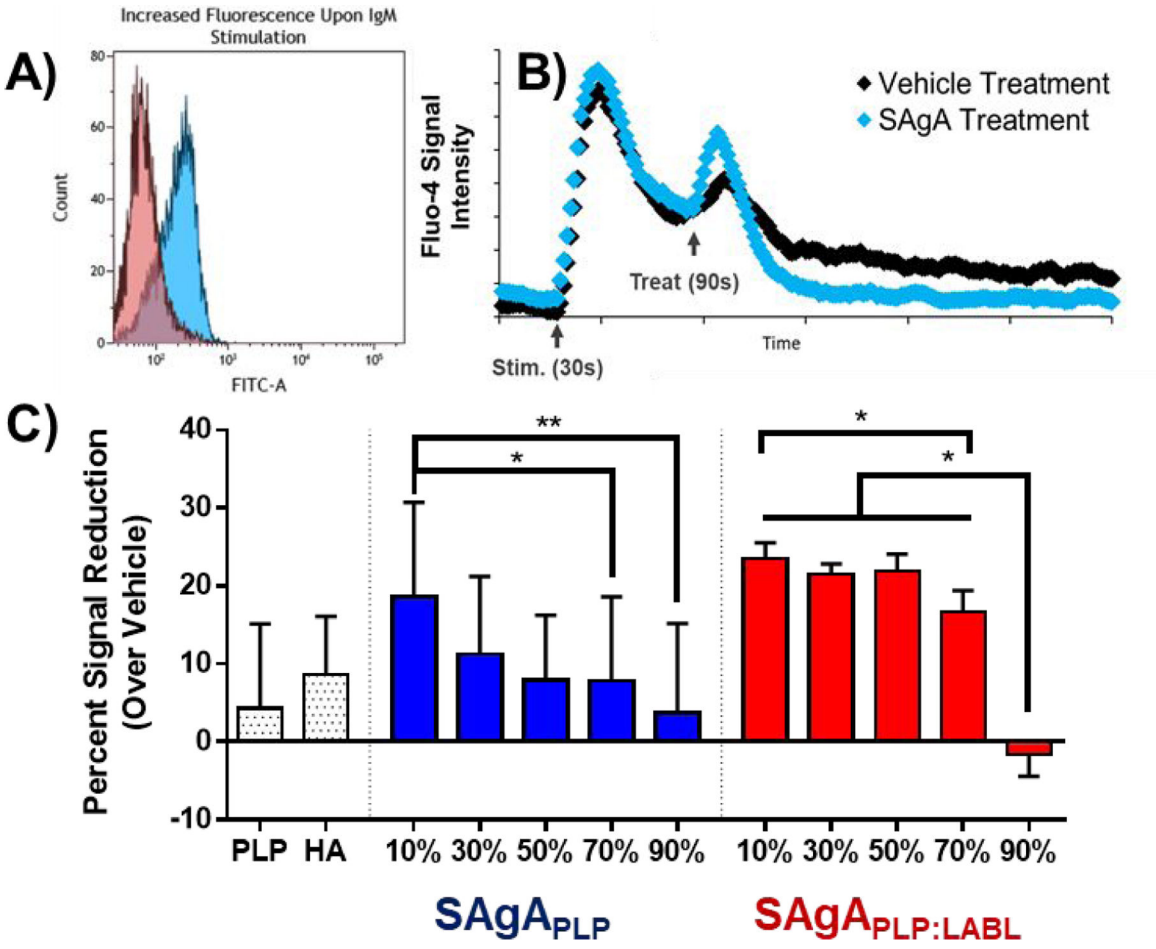

Fig. 2.

Calcium flux was used as a measure of acute B-cell response by varied valency conjugates. **A)** Raji B-cells were loaded with Fluo-4 as a fluorescent calcium indicator and stimulated with IgM. Fluo-4 signal was increased from baseline (left) after stimulation (right). **B)** Acute B-cell inhibition was measured by stimulating Raji B-cells for 60 s, followed by treatment with varied valency conjugates. After treatment, mean fluorescence intensity was monitored for 180s and compared to the 60 second stimulation period. **C)** Reduced calcium signaling by one-signal varied valency conjugates ($SAgA_{PLP}$, blue), two-signal varied valency conjugates ($SAgA_{PLP:LABL}$, red), monovalent PLP and azide-modified HA alone (white). (n > 3/group, *p < 0.05, **p < 0.01).

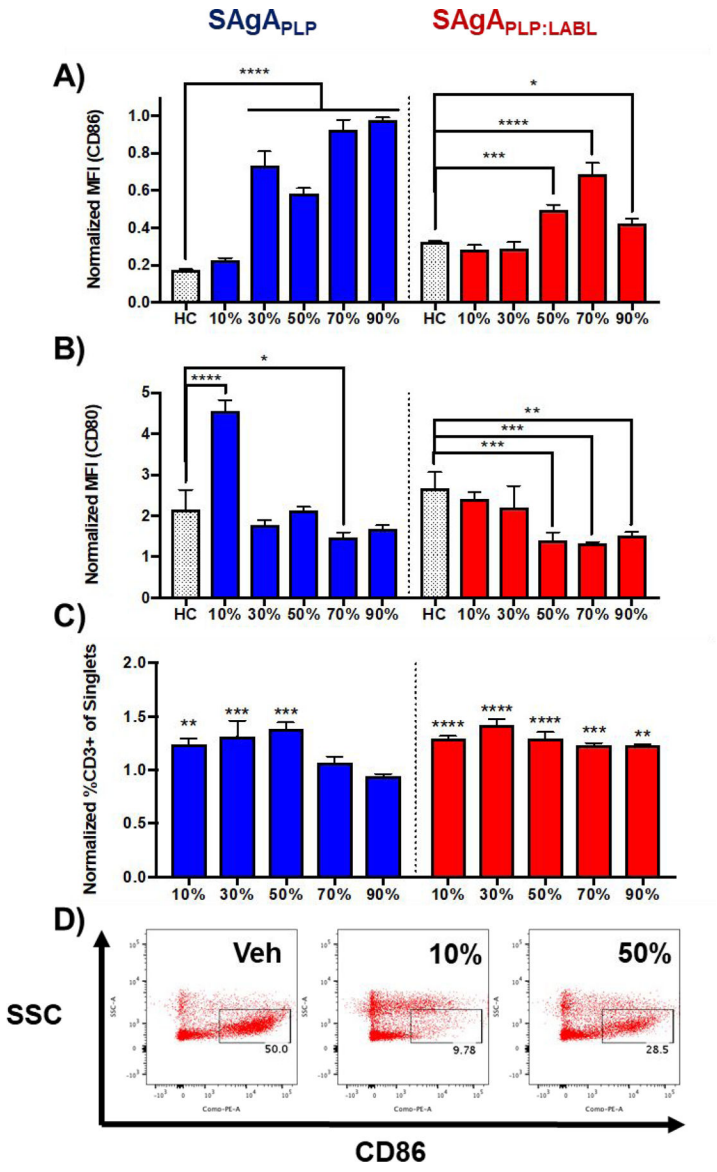

Fig. 3.

Mixed splenocytes were harvested from EAE mice at peak of disease, treated with varied valency conjugates, and rechallenged with 25 μM PLP for 72h. Following the incubation, cells were fluorescently labeled and analyzed by flow cytometry, where changes in **A)** CD86, **B)** CD80, and **C)** CD3 were compared to healthy control splenocytes (HC). All values are expressed in terms of fold-change as compared to vehicle treated EAE splenocytes. **D)** CD86 changes are shown by dot plot for PBS-treated EAE spenocytes, as well as those treated with low-valency SAgA$_{PLP:LABL}$ or SAgA$_{PLP:LABL}$ of typical valency from previous reports. (n = 3/group, *p < 0.05, **p < 0.01, ***p < 0.001, ****p < 0.0001).

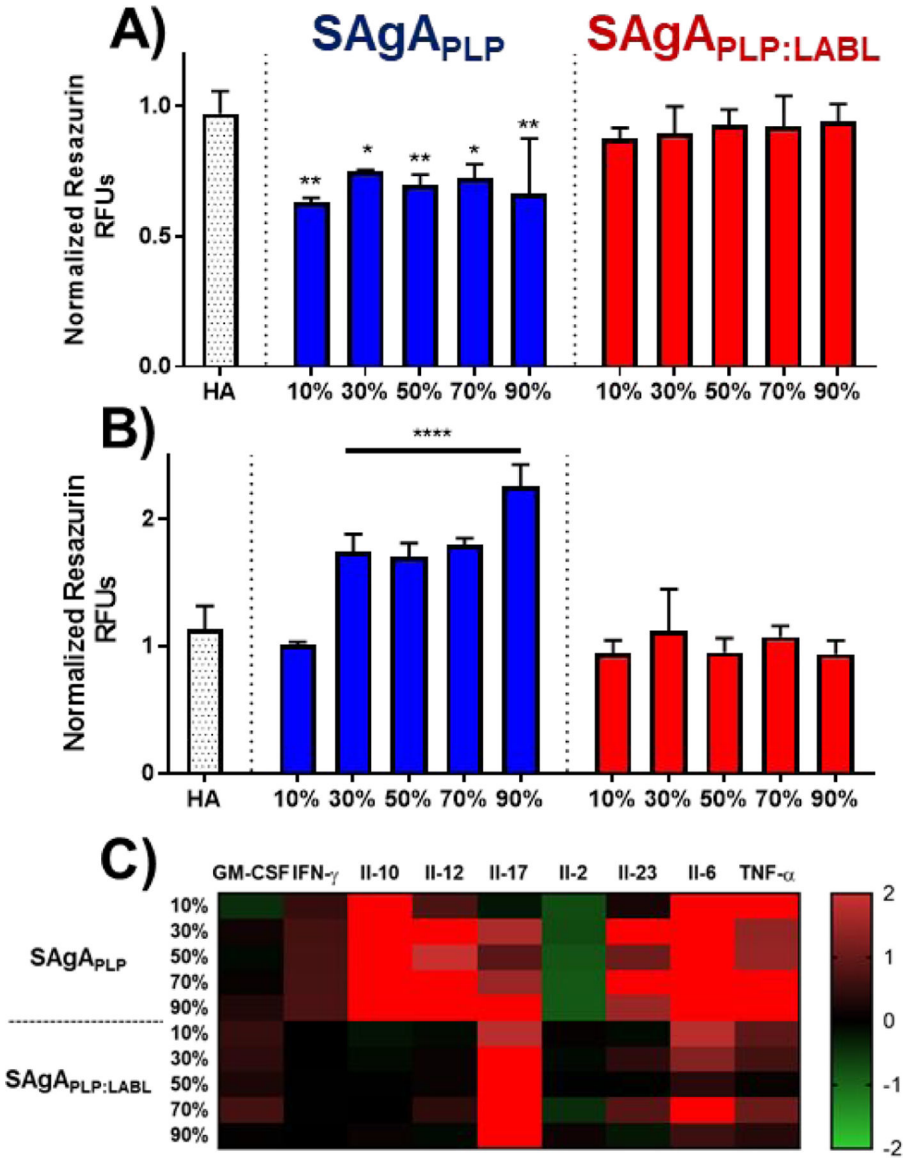

Fig. 4.

A) EAE splenocytes treated with varied valency conjugates and 25 μM PLP rechallenge. Groups were incubated with resazurin after 72 hr to assess differences in cell metabolism. **B)** Likewise, healthy splenocytes were treated with varied valency conjugates and 25 μM PLP and subsequently incubated with resazurin after 72 hr. **C)** Supernatants were collected from conjugate-treated EAE splenocytes and analyzed for GM-CSF, IFN- γ, Il-10, Il-12, Il-17, Il-2, Il-23, Il-6, and TNF-α. (n = 3/group, *p < 0.05, **p < 0.01, ***p < 0.001, ****p < 0.0001).

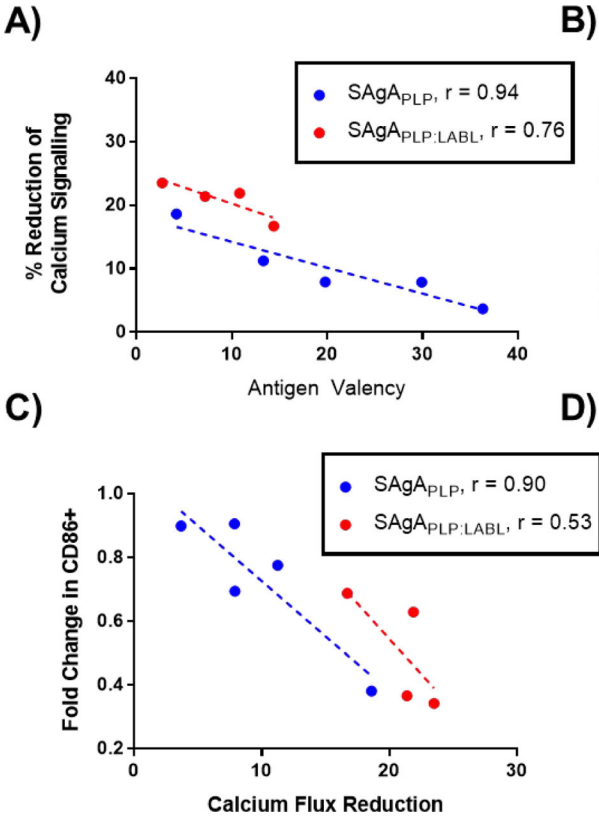

D)

	Pearson Correlation Coefficient, r
Calcium Flux Reduction vs. PLP Valency	-0.88 (p = 0.0007)
Fold Change in CD86+ vs. PLP Valency	0.83 (p = 0.003)
Fold Change in CD86+ vs. Calcium Flux Reduction	-0.84 (p = 0.002)

Fig. 5.

Inhibitory outcomes from treating EAE splenocytes with varied valency conjugates were assessed according to PLP valency, including **A)** acute inhibition of B-cells and **B)** CD86 expression. Pearson correlation coefficients were calculated for each comparison. **C)** Correlation between acute B-cell inhibition and downstream CD86+ expression was also investigated. **D)** The relationship between PLP valency, calcium flux reduction, and CD86 expression changes was collectively analyzed to form a correlation matrix where Pearson correlation coefficients were expressed. In Figures 5A and 5C, data points for 90% SAgA$_{PLP:LABL}$ are omitted for clarity, but readouts from this group are applied for the analysis in Figures 5D.